Solid state ^{29}Si NMR studies of apatite-type oxide ion conductors

Jonathan E. H. Sansom,[a] Julian R. Tolchard,†[a] M. Saiful Islam,‡[a] David Apperley[b] and Peter R. Slater*[a]

Received 5th January 2006, Accepted 10th February 2006
First published as an Advance Article on the web 17th February 2006
DOI: 10.1039/b600122j

Apatite-type silicates have been attracting considerable interest as a new class of oxide ion conductor, whose conduction is mediated by interstitial oxide ions. We report here the first ^{29}Si solid state NMR studies of these materials with a systematic investigation of thirteen compositions. Our results indicate a correlation between the silicon environment and the observed conductivity. Specifically, samples which show poor conductivity demonstrate a single NMR resonance, whereas fast ion conducting compositions show more complex NMR spectra. For the oxygen excess samples $La_9M(SiO_4)_6O_{2.5}$ (M = Ca, Sr, Ba) two peaks are observed at chemical shifts of ≈ -77.5 and -80.5 ppm, with the second peak correlated with a silicate group adjacent to an interstitial oxygen site. On Ti doping to give $La_9M(SiO_4)_{6-x}(TiO_4)_xO_{2.5}$ (x = 1,2) the second peak disappears, which is consistent with the "trapping" of interstitial oxygens by Ti and the consequent lowering in oxide ion conductivity. The samples $La_{9.33}(SiO_4)_6O_2$ and $La_{9.67}(SiO_4)_6O_{2.5}$ show a further third weak peak at a chemical shift (≈ -85.0 ppm) consistent with the presence of some $[Si_2O_7]^{6-}$ units in these samples, due to condensation of two $[SiO_4]^{4-}$ units. The effect of such condensation of $[SiO_4]^{4-}$ units will be the creation of additional interstitial oxide ion defects, *i.e.* $2\ [SiO_4]^{4-} \rightarrow [Si_2O_7]^{6-} + O_{int}^{2-}$. Overall, the results further highlight the importance of the $[SiO_4]^{4-}$ substructure in these materials, and additionally suggest that ^{29}Si NMR could potentially be used to screen apatite silicate materials for oxide ion conductivity

Introduction

Materials showing high oxide ion conductivity have been attracting considerable attention due to applications in a range of areas including solid oxide fuel cells, oxygen sensors and separation membranes. In the area of solid oxide fuel cells, the conventional electrolyte is yttria stabilised zirconia (YSZ). This is an excellent electrolyte material as it exhibits negligible electronic conduction over a wide range of $p(O_2)$., and provides a good thermal expansion match with current cell component technologies. However, in order to achieve sufficient oxide ion conductivity, very high temperatures (~1000 °C) are required. There is therefore considerable interest in developing alternative electrolytes with lower operating temperatures, and in this respect several groups have reported promising results for the lanthanide silicate/germanate apatite systems, $Ln_{10-x}(Si/GeO_4)_6O_{2+y}$ (Ln = lanthanide).[1–6] The general structure of these materials consists of isolated Si/GeO_4 units with the lanthanide cations located in two types of channel sites, with 9-fold and 7-fold coordination. The non-silicate/germanate oxygen ions occupy one-dimensional channels running through the structure (Fig. 1).

There is now a significant body of work relating to these systems, most with the focus on understanding and optimising the oxide ion conductivity (see review in ref. 7 and references therein). It is now well established that fully stoichiometric systems, *e.g.* $La_8Sr_2(SiO_4)_6O_2$, have much lower conductivities and higher activation energies than systems containing either cation vacancies, *e.g.* $La_{9.33}(SiO_4)_6O_2$, or oxygen excess, *e.g.* $La_9Sr(SiO_4)_6O_{2.5}$. This has been attributed to fast oxide ion conductivity proceeding *via* oxide ion interstitials.[5–8] This contrasts with the conventional fluorite (*e.g.* YSZ) or perovskite (*e.g.* $La_{1-x}Sr_xGa_{1-y}Mg_yO_{3-x/2-y2}$) materials, which are well known oxide ion vacancy conductors.

In our previous studies, we investigated the mechanism of oxide ion migration for two typical apatite compositions,

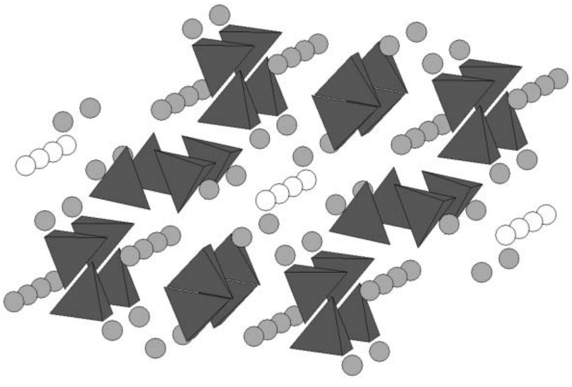

Fig. 1 The apatite structure, $Ln_{10-x}(Si/GeO_4)_6O_{2+y}$ (dark spheres = Ln, tetrahedra = Si/GeO_4, light spheres = O).

---

[a] *Chemistry, UniS Materials Institute, University of Surrey, Guildford, Surrey, UK, GU2 7XH. E-mail: p.slater@surrey.ac.uk; Fax: +44 1483 686851; Tel: +44 1483 686847*
[b] *Department of Chemistry, Durham University, South Road, Durham, UK, DH1 3LE*

† Present address: Department of Materials Technology, Norwegian University of Science and Technology, Sem Sælands vei 14, N-7491 Trondheim, Norway.

‡ Present address: Department of Chemistry, University of Bath, Bath, UK BA2 7AY.

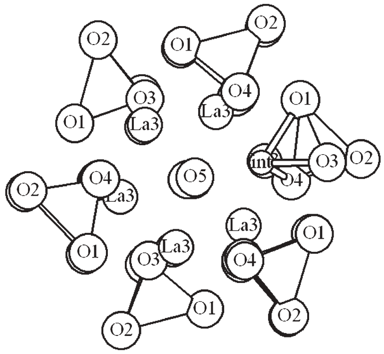

Fig. 2 The local environment around the oxide ion channels in the apatite structure (tetrahedral = Si/GeO$_4$). The interstitial oxygen position (int) lies at the periphery of the channel, and is accommodated by a displacement of the adjacent Si/GeO$_4$ tetrahedra.

$La_{9.33}(SiO_4)_6O_2$ (a good conductor) and $La_8Sr_2(SiO_4)_6O_2$ (a poor conductor), *via* atomistic modelling.[8,9] Our results predicted that oxide ion conduction proceeds *via* an interstitial mechanism in $La_{9.33}(SiO_4)_6O_2$, while for $La_8Sr_2(SiO_4)_6O_2$ the mechanism involved migration of oxygen vacancies. The modelling studies also predicted the presence of an energetically favourable oxygen interstitial position located at the periphery of the channels (Fig. 2), and highlighted the important role played by relaxation of the $[SiO_4]^{4-}$ substructure in the fast ion conductivity in apatite systems. Experimental support for the presence of these interstitial oxide ions has since come from structural studies of oxygen excess systems, $La_{9.33+x}(Si/GeO_4)_6O_{2+3x/2}$, and Mössbauer studies of Fe doped samples.[10–13] In particular, structural studies by Leon-Reina *et al.* have confirmed the correlation between high conductivity and the presence of these interstitial oxide ions at the channel periphery.[13]

Despite the large interest in these materials, their structural complexity means that they are still not fully characterised. For example, although results from single crystal studies of $Ln_{9.33}(SiO_4)_6O_2$ (Ln = Pr, Nd, Sm) have confirmed that the conductivity is anisotropic, being greatest parallel to *c* (the direction of the oxygen channels),[4] the observed enhancement ($\approx$one order of magnitude) is not as high as might be expected considering the one-dimensional nature of these oxygen channels. Moreover, the activation energies for conduction along *a*, *b*, and *c* are fairly similar, suggesting that although the main conduction pathway is down the oxide ion channels, there is also significant conduction perpendicular to the channels, which needs to be accounted for. With this in mind, we have collected ^{29}Si NMR data on a range of samples, in order to further investigate the role of the $[SiO_4]^{4-}$ substructure in the fast oxide ion conduction of these materials

Experimental

A selection of 11 samples was initially prepared (Table 1) to include samples which were poorly conducting and those showing high conductivities (both samples containing cation vacancies and/or oxygen excess). The samples were prepared from high purity La_2O_3, $BaCO_3$, $SrCO_3$, $CaCO_3$, SiO_2, which were intimately mixed in the correct ratios and heated to 1300 °C for 14 hours, reground and then reheated to 1300–1400 °C for a further 14 hours. Phase purity was confirmed using X-ray powder diffraction (Seifert 3003TT diffractometer). Subsequently two further Ti doped samples, $La_9Ba(SiO_4)_{6-x}(TiO_4)_xO_{2.5}$ (x = 1, 2) were prepared, utilising TiO_2 as a starting material, and synthesis temperatures of 1300 °C for 14 hours, followed by 1500 °C for a further 14 hours.

Table 1 Apatite oxide samples studied, along with their conductivities at 800 °C

Sample	Conductivity at 800 °C/S cm^{-1}	Defect structure
$La_{9.33}(SiO_4)_6O_2$	2.0×10^{-3}	Cation vacancies
$La_{8.67}Ca(SiO_4)_6O_2$	1.5×10^{-3}	Cation vacancies
$La_{8.67}Sr(SiO_4)_6O_2$	1.5×10^{-3}	Cation vacancies
$La_{8.67}Ba(SiO_4)_6O_2$	1.7×10^{-3}	Cation vacancies
$La_{9.67}(SiO_4)_6O_{2.5}$	0.01	Cation vacancies and oxygen excess
$La_9Ca(SiO_4)_6O_{2.5}$	0.02	Oxygen excess
$La_9Sr(SiO_4)_6O_{2.5}$	0.01	Oxygen excess
$La_9Ba(SiO_4)_6O_{2.5}$	0.05	Oxygen excess
$La_8Ca_2(SiO_4)_6O_2$	9.9×10^{-7}	Fully stoichiometric
$La_8Sr_2(SiO_4)_6O_2$	5.6×10^{-7}	Fully stoichiometric
$La_8Ba_2(SiO_4)_6O_2$	5.4×10^{-7}	Fully stoichiometric

Solid state NMR data were collected on a Varian Unity Inova spectrometer operating at 59.56 MHz for ^{29}Si and with a 7.5 mm (rotor o.d.) MAS probe. Direct-polarisation experiments with a 5 microsecond 90° pulse and recycle delays of between 30 and 300 s were used with sample spin-rates of 5 kHz. Chemical shifts are quoted relative to tetramethylsilane. Intensity information was obtained by spectral deconvolution.

Results and discussion

The ^{29}Si NMR data are summarised in Table 2 with example spectra shown in Fig. 3 and 4. For the samples containing alkaline earth (Ca, Sr, Ba) doping, the ^{29}Si NMR data showed that all the samples which were fully stoichiometric, $La_8M_2(SiO_4)_6O_2$ (M = Ca, Sr, Ba), exhibited a single ^{29}Si NMR peak, whereas samples which were cation deficient, $La_{8.67}M(SiO_4)_6O_2$ or contained oxygen excess, $La_9M(SiO_4)_6O_{2.5}$ showed two peaks, one at a similar position to the stoichiometric samples, with the second at a more

Table 2 ^{29}Si NMR peak positions for a range of silicate apatite materials

Sample	Peak positions (ppm)	Relative intensities (%)
$La_{9.33}(SiO_4)_6O_2$	−77.8, −81.0, −85.3	53.8, 38.4, 7.8
$La_{8.67}Ca(SiO_4)_6O_2$	−77.4, −80.5	75.1, 24.9
$La_{8.67}Sr(SiO_4)_6O_2$	−77.5, −80.6	71.7, 28.3
$La_{8.67}Ba(SiO_4)_6O_2$	−77.8, −80.6	70.5, 29.5
$La_{9.67}(SiO_4)_6O_{2.5}$	−77.7, −80.7, −85.1	52.2, 42.6, 5.2
$La_9Ca(SiO_4)_6O_{2.5}$	−77.4, −80.5	69.8, 30.2
$La_9Sr(SiO_4)_6O_{2.5}$	−77.5, −80.5	71.3, 28.7
$La_9Ba(SiO_4)_6O_{2.5}$	−77.9, −80.8	79.1, 20.9
$La_8Ca_2(SiO_4)_6O_2$	−77.2	100
$La_8Sr_2(SiO_4)_6O_2$	−77.8	100
$La_8Ba_2(SiO_4)_6O_2$	−78.3	100

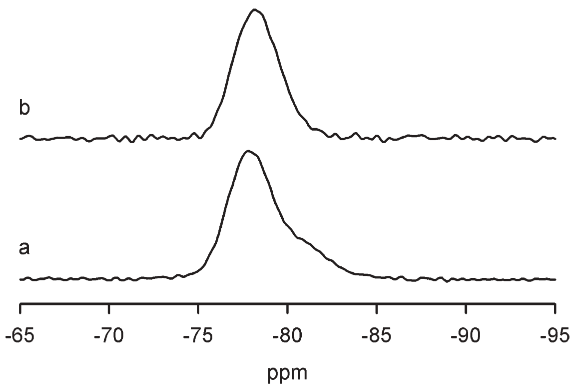

Fig. 3 ^{29}Si NMR spectra for (a) $La_{8.67}Ba(SiO_4)_6O_2$ (246 repetitions with 300 s recycle delay) showing two overlapping peaks, one at chemical shift = −77.8 ppm with the other at −80.6 ppm; (b) $La_8Ba_2(SiO_4)_6O_2$ (289 repetitions with 300 s recycle delay) showing a single peak at chemical shift = −78.3 ppm.

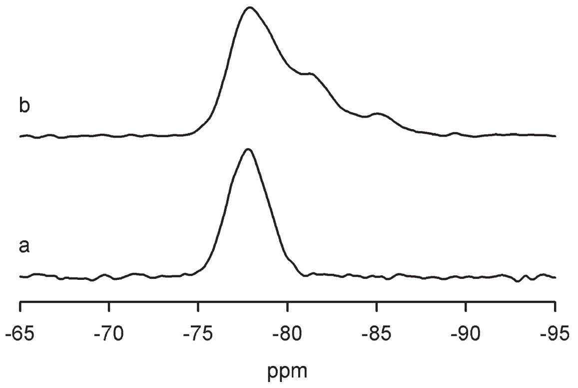

Fig. 4 ^{29}Si NMR spectra for (a) $La_8Sr_2(SiO_4)_6O_2$ (200 repetitions with 300 s recycle delay) showing a single peak at chemical shift = −77.8 ppm; (b) $La_{9.33}(SiO_4)_6O_2$ (180 repetitions with 300 s recycle delay) showing three overlapping peaks, at chemical shifts of −77.8, −81.0 and −85.3 ppm.

negative chemical shift. For the two samples without alkaline earth dopants, $La_{9.33}(SiO_4)_6O_2$ and $La_{9.67}(SiO_4)_6O_{2.5}$, a third weaker peak at even lower chemical shift was observed (Table 2).

As highlighted in previous studies, the apatite structure is somewhat complex,[7] and the presence of defects, whether as dopants, cation vacancies, or interstitial oxide ions, is likely to cause significant changes in the local structure.[8,9,14] It is therefore important to consider the effect of all these possible defects in interpreting the NMR data.

The chemical shifts for the ^{29}Si NMR data presented in Table 2 are generally consistent with the established apatite structure incorporating isolated tetrahedral $[SiO_4]^{4-}$ units. The presence of more than one resonance for some compositions indicates that not all $[SiO_4]^{4-}$ units are equivalent, most likely due to distortions and/or displacements of some $[SiO_4]^{4-}$ groups by dopants, cation vacancies or oxygen interstitials.

It can be seen that the poorly conducting, fully stoichiometric, $La_8M_2(SiO_4)_6O_2$ (M = Ca, Sr, Ba) samples show a single Si peak, and hence single Si environment. This suggests that the silicate sublattice is quite uniform in these samples. It also indicates that the additional peak in the cation deficient, $La_{8.67}M(SiO_4)_6O_2$, and oxygen excess, $La_9M(SiO_4)_6O_{2.5}$, samples is unlikely to be correlated with the effect of the divalent dopants (Ca, Sr, Ba), since a similar peak would have been expected for the $La_8M_2(SiO_4)_6O_2$ samples.

Therefore the extra ^{29}Si NMR peak(s) observed for samples with cation vacancies and/or oxygen excess likely arise from the effect of cation vacancies and oxygen interstitials on the silicate network. Atomistic simulation studies have shown that both defects cause similar large disruption to the $[SiO_4]^{4-}$ units.[8,9,14] It is therefore difficult to conclusively correlate the extra peak at chemical shift ≈ −80.5 ppm to only one of these defects, as both are likely to contribute to the local distortions of the Si environment. However, the fact that there are no cation vacancies in the oxygen excess samples, $La_9M(SiO_4)_6O_{2.5}$, means that in these particular samples, a correlation between the extra Si site and the presence of neighbouring interstitial oxygen can be proposed.

The origin of the third peak at chemical shift ≈ −85.0 ppm in the samples $La_{9.33}(SiO_4)_6O_2$ and $La_{9.67}(SiO_4)_6O_{2.5}$ is interesting. The chemical shift of this peak is more typical of a Q^1 signal rather than the Q^0 signal that is expected for the isolated $[SiO_4]^{4-}$ groups in the apatite structure.[15] This therefore suggests the presence of some $[Si_2O_7]^{6-}$ units in these samples, due to condensation of two $[SiO_4]^{4-}$ units. Such condensation may arise from the large structural distortions, caused by the presence of high levels of cation vacancies ($La_{9.33}(SiO_4)_6O_2$) or cation vacancies and oxygen excess ($La_{9.67}(SiO_4)_6O_{2.5}$), bringing two $[SiO_4]^{4-}$ groups close together. A further effect of such condensation of $[SiO_4]^{4-}$ units will be the creation of additional interstitial oxide ion defects, *i.e.* $2\,[SiO_4]^{4-} \rightarrow [Si_2O_7]^{6-} + O_{int}{}^{2-}$. Furthermore, the influence of such condensation on the local structure may be to create additional pathways for conduction between channels leading to higher than expected conductivity perpendicular to the channels, as observed from single crystal studies of $Ln_{9.33}(SiO_4)_6O_2$ (Ln = Pr, Nd, Sm).[4]

Overall the results above show that samples with high conductivity display greater structural disorder of the silicate sublattice, and provide further experimental confirmation of modelling predictions that the silicate sublattice plays a critical role in the conduction process.

As an additional experiment, two further Ti doped oxygen excess samples, $La_9Ba(SiO_4)_4(TiO_4)_2O_{2.5}$ and $La_9.Ba(SiO_4)_5(TiO_4)O_{2.5}$, were examined. These samples were chosen as Ti doping has been shown to significantly decrease the oxide ion conductivity even in samples containing oxygen excess.[16] The conductivity of $La_9Ba(SiO_4)_4(TiO_4)_2O_{2.5}$ is nearly three orders of magnitude lower than that of $La_9Ba(SiO_4)_6O_{2.5}$ (Tables 1, 3).

Table 3 ^{29}Si NMR data and conductivities for Ti doped apatite samples

Sample	Conductivity at 800 °C/S cm^{-1}	^{29}Si NMR peak position (relative intensity)
$La_9.Ba(SiO_4)_5(TiO_4)O_{2.5}$	1.9×10^{-4}	−78.1 ppm (100%)
$La_9Ba(SiO_4)_4(TiO_4)_2O_{2.5}$	7.2×10^{-5}	−78.0 ppm (100%)

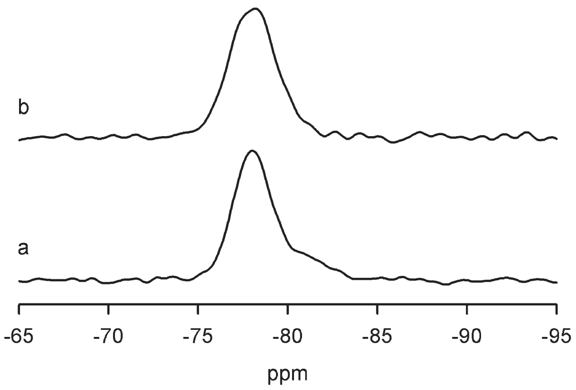

Fig. 5 ^{29}Si NMR spectra for (a) $La_9Ba(SiO_4)_6O_{2.5}$ (196 repetitions with 300 s recycle delay) showing two overlapping peaks, one at chemical shift = −77.9 ppm with the other at −80.8 ppm; (b) $La_9Ba(SiO_4)_4(TiO_4)_2O_{2.5}$ (80 repetitions with 120 s recycle delay) showing a single peak at chemical shift = −78.0 ppm.

The ^{29}Si NMR results for these two Ti doped oxygen excess samples (Table 3) showed the same single peak as the poorly conducting samples, $La_8M_2(SiO_4)_6O_2$ (M = Ca, Sr, Ba). This contrasts with the $La_9Ba(SiO_4)_6O_{2.5}$ parent composition, which showed two Si environments (Fig. 5), and is consistent with the hypothesis that interstitial oxide ions are "trapped" by Ti increasing its coordination sphere.[16] Moreover, it adds weight to the above interpretation that the extra NMR peak at −80.8 ppm in $La_9Ba(SiO_4)_6O_{2.5}$ is associated with a silicate unit near an interstitial oxygen position, and that these interstitial oxide ions are important in the conduction process.

In conclusion, ^{29}Si NMR results for a range of apatite-type oxide ion conductors have shown that in poorly conducting samples, the silicate sublattice is uniform, as evidenced by a single NMR resonance. In contrast, highly conducting samples exhibit more than one Si environment. This is attributed to local distortions caused by the presence of interstitial oxygens and cation vacancies. The results further highlight the importance of the $[SiO_4]^{4-}$ substructure in the fast oxide ion conduction process, and additionally suggest that ^{29}Si NMR could potentially be used to screen apatite silicate materials for oxide ion conductivity: samples showing more than one peak in the ^{29}Si NMR spectrum being expected to show good conductivity.

Acknowledgements

We would like to thank EPSRC for funding. We would also like to thank the EPSRC solid-state NMR service for data collection.

References

1 S. Nakayama, T. Kagayama, H. Aono and Y. Sadoaka, *J. Mater. Chem.*, 1995, **5**, 1801.
2 H. Arikawa, N. Nishiguchi, T. Ishihara and Y. Takita, *Solid State Ionics*, 2000, **136–137**, 31.
3 S. Nakayama, M. Sakamoto, M. Higuchi, K. Kodaira, M. Sato, S. Kakita, T. Suzuki and K. Itoh, *J. Eur. Ceram. Soc.*, 1999, **19**, 507.
4 S. Nakayama, M. Sakamoto, M. Highchi and K. Kodaira, *J. Mater. Sci. Lett.*, 2000, **19**, 91; S. Nakayama and M. Niguchi, *J. Mater. Sci. Lett.*, 2001, **20**, 913.
5 J. E. H. Sansom, D. Richings and P. R. Slater, *Solid State Ionics*, 2001, **139**, 205.
6 A. Najib, J. E. H. Sansom, J. R. Tolchard, M. S. Islam and P. R. Slater, *Dalton Trans.*, 2004, 3106.
7 P. R. Slater, J. E. H. Sansom and J. R. Tolchard, *Chem. Rec.*, 2004, **4**, 373.
8 M. S. Islam, J. R. Tolchard and P. R. Slater, *Chem. Commun.*, 2003, 1486.
9 J. R. Tolchard, M. S. Islam and P. R. Slater, *J. Mater. Chem.*, 2003, **13**, 1956.
10 L. León-Reina, M. C. Martín-Sedeño, E. R. Losilla, A. Cabeza, M. Martínez-Lara, S. Bruque, F. M. B. Marques, D. V. Sheptyakov and M. A. G. Aranda, *Chem. Mater.*, 2003, **15**, 2099.
11 L. León-Reina, E. R. Losilla, M. Martínez-Lara, S. Bruque and M. A. G. Aranda, *J. Mater. Chem.*, 2004, **14**, 1142.
12 A. L. Shaula, V. V. Kharton, J. C. Waerenborgh, D. P. Rojas, E. V. Tsipis, N. P. Vyshatko, M. V. Patrakeev and F. M. B. Marques, *Mater. Res. Bull.*, 2004, **39**, 763.
13 L. Leon-Reina, E. R. Losilla, M. Martinez-Lara, S. Bruque, A. Llobet, D. V. Sheptyakov and M. A. G. Aranda, *J. Mater. Chem.*, 2005, **15**, 2489.
14 J. R. Tolchard, P. R. Slater and M. S. Islam, manuscript in preparation.
15 E. Lippmaa, M. Magi, A. Samoson, G. Engelhardt and A. R. Grimmer, *J. Am. Chem. Soc.*, 1980, **102**, 4889.
16 J. E. H. Sansom, P. A. Sermon and P. R. Slater, *Solid State Ionics*, 2005, **176**, 1765.